AD-A043 025 PENNSYLVANIA STATE UNIV UNIVERSITY PARK APPLIED RESE--ETC F/G 20/4
ROTOR INCOMING VELOCITY PROFILE MEASUREMENTS.(U)
OCT 76 M L BILLET N00017-73-C-1418
UNCLASSIFIED TM-76-254 NL

1 OF 1
ADA043025

END
DATE FILMED
9-77
DDC

The Pennsylvania State University
Institute for Science and Engineering
APPLIED RESEARCH LABORATORY
Post Office Box 30
State College, Pa. 16801

NAVY DEPARTMENT

NAVAL SEA SYSTEMS COMMAND

ROTOR INCOMING VELOCITY PROFILE MEASUREMENTS

M. L BILLET

Technical Memorandum
File No. TM 76-254
11 October 1976
Contract No. N00017-73-C-1418

Copy No. _____

The Pennsylvania State University
APPLIED RESEARCH LABORATORY
Post Office Box 30
State College, PA 16801

PREPARED UNDER THE NAVAL SEA SYSTEMS COMMAND GENERAL HYDROMECHANICS RESEARCH PROGRAM ADMINISTERED BY THE DAVID W. TAYLOR NAVAL SHIP RESEARCH AND DEVELOPMENT CENTER (CODE 1505), BETHESDA, MD 20084

UNCLASSIFIED

SECURITY CLASSIFICATION OF THIS PAGE (When Data Entered)

REPORT DOCUMENTATION PAGE

READ INSTRUCTIONS BEFORE COMPLETING FORM

1. REPORT NUMBER: TM-76-254	2. GOVT ACCESSION NO.
3. RECIPIENT'S CATALOG NUMBER	
4. TITLE (and Subtitle): ROTOR INCOMING VELOCITY PROFILE MEASUREMENTS.	5. TYPE OF REPORT & PERIOD COVERED: Technical Memorandum
6. PERFORMING ORG. REPORT NUMBER	
7. AUTHOR(s): M. L. Billet	8. CONTRACT OR GRANT NUMBER(s): N00017-73-C-1418
9. PERFORMING ORGANIZATION NAME AND ADDRESS: Applied Research Laboratory, P. O. Box 30, State College, PA 16801	10. PROGRAM ELEMENT, PROJECT, TASK AREA & WORK UNIT NUMBERS
11. CONTROLLING OFFICE NAME AND ADDRESS: Naval Sea Systems Command, Washington, DC 20362	12. REPORT DATE: 11 October 1976
	13. NUMBER OF PAGES: 45
14. MONITORING AGENCY NAME & ADDRESS (if different from Controlling Office): 48p.	15. SECURITY CLASS. (of this report): UNCLASSIFIED
	15a. DECLASSIFICATION/DOWNGRADING SCHEDULE

16. DISTRIBUTION STATEMENT (of this Report)

Approved for public release. Distribution unlimited.
Per NAVSEA -

17. DISTRIBUTION STATEMENT (of the abstract entered in Block 20, if different from Report)

18. SUPPLEMENTARY NOTES

19. KEY WORDS (Continue on reverse side if necessary and identify by block number)

Flow
Rotor
Boundary Layer
Wind Tunnel
Vorticity

20. ABSTRACT (Continue on reverse side if necessary and identify by block number)

Boundary layer profiles were measured for various flow conditions at a position in front of a rotor. The rotor was located at the downstream end on an axisymmetric body. Results were obtained with/without upstream appendages, with/without upstream screen, and for on design/off design rotor flow coefficients. All tests were conducted in the 48-inch diameter wind tunnel at a nominal velocity of 80 fps.

DD FORM 1 JAN 73 1473 EDITION OF 1 NOV 65 IS OBSOLETE

391 007

UNCLASSIFIED

SECURITY CLASSIFICATION OF THIS PAGE (When Data Entered)

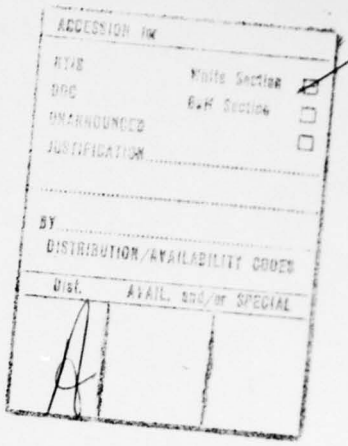

From: M. L. Billet

Subject: Rotor Incoming Velocity Profile Measurements

References: See page 17.

Abstract: Boundary layer profiles were measured for various flow conditions at a position in front of a rotor. The rotor was located at the downstream end on an axisymmetric body. Results were obtained with/without upstream appendages, with/without upstream screen, and for on design/off design rotor flow coefficients. All tests were conducted in the 48-inch diameter wind tunnel at a nominal velocity of 80 fps.

Acknowledgments: This report is based upon research conducted under the General Hydromechanics Research Program of the Naval Ship Systems Command, technically administered by the David Taylor Naval Ship Research and Development Center.

The author would like to thank Donald E. Thompson whose wind tunnel experimental set-up was used in this test.

Table of Contents

List of Tables

11 October 1976
MLB:jep

List of Figures

List of Figures (Cont.)

11 October 1976
MLB:jep

Nomenclature

A - constant of 5.76

B - constant of 5.5

C_f - skin friction coefficient

H - axisymmetric shape factor

$\overline{H}$ - planar shape factor

k - von Karman constant of 0.4

m - power law exponent

R - Reynolds number, $\frac{U \cdot D}{\nu}$

R_R - dius of rotor

R_θ - ynolds number, $R_\theta = \frac{U\overline{\theta}}{\nu}$

U_e - velocity at edge of boundary layer

u - velocity

u^+ - nondimensional mean velocity $u^+ = u/u^*$

u^* - shear velocity $u^* = \sqrt{\tau_w/\rho}$

V_∞ - free stream velocity

W - relative velocity

Y - normal distance from wall

y^+ - nondimensional distance from wall, $y^+ = \frac{u^* Y}{\nu}$

ω_s' - relative streamwise vorticity

ω_n' - relative normal vorticity

θ_c - relative camber angle

$\overline{\delta}^*$ - planar displacement thickness

$\overline{\theta}$ - planar momentum

$\overline{\delta}$ - planar boundary thickness

Nomenclature (Cont.)

δ^* - axisymmetric displacement thickness

θ - axisymmetric momentum thickness

δ - axisymmetric boundary layer thickness

α - defined by Equation (9)

ϕ - angle between axis of symmetry and tangent to surface

ρ - density of fluid

ν - kinematic viscosity of fluid

INTRODUCTION

The experimental results presented in this paper were obtained as part of an investigation of secondary flows produced in the blade passage of a rotor. As shown by many investigators [1,2]*, the amount of secondary streamwise vorticity produced at the blade exit plane (ω'_{s_2}) depends primarily on the slope of the incoming boundary layer to the rotor ($\omega_{n_1} = \frac{dU}{dY}$) and the blade loading (θ_c). Any knowledge of the shape of the incoming velocity profile to the rotor is valuable in calculating not only the secondary flows but also the rotor primary flow. Such factors as body length and upstream appendages couple with the rotor effects to influence the profile of the incoming boundary layer. Near the end of an axisymmetric body where the rotor is located, significant changes occur in the boundary layer profile because the radii of curvature is the order of the boundary layer thickness.

Many investigators such as Patel [3,4] and Granville [5] have developed methods to calculate the momentum thickness of a turbulent boundary layer on an axisymmetric body without a rotor. In particular, Patel [3] has an integral method which includes the effect of transverse radius of curvature which produces an interaction such that the static pressure does not remain constant across the boundary layer. This effect can be important over as much as the last 30% of the body length.

This report presents detailed boundary layer measurements near the body in a plane located in front of the rotor. These measurements were made for various rotor operating flow coefficients and varying upstream body configurations. The measured profiles are compared with basic boundary layer relationships.

---

*Numbers in brackets refer to documents in references.

DESCRIPTION OF EXPERIMENTS

Tests were conducted in the 48-inch diameter wind tunnel located in the Garfield Thomas Water Tunnel Building at the Pennsylvania State University at a nominal velocity of 80 fps which corresponds to a Reynolds number of 3.0×10^5 based on rotor diameter. This velocity was chosen to insure turbulent flow over the forebody. The rotor was located near the end of an axisymmetric body where the boundary layer thickness is large and is the same order of magnitude as the body curvature.

Results were obtained with/without appendages, with/without a screen on the nose of the axisymmetric forebody, and on/off design rotor flow coefficients. These basic flows are described in Table 1. Basic flow No. 11 (without appendages, screen, and rotor) is the most amenable to theoretical boundary layer analysis.

To minimize any effects produced by tunnel-wall interference, a "liner" was used in the test section. The resulting inner contour in the test section was determined by a potential flow solution for the body which approximated a stream surface where the body is in a flow of infinite extent.

Total pressure tubes and static pressure tubes were positioned in front of the rotor. Figure 1 is a schematic of the test configuration. In all, three total pressure rakes and one static pressurerake were used. As the rakes were rotated, pressures were recorded at two degree increments for a total of 360 degrees. In addition, static pressures were obtained on the surface of the model at the various locations shown in Figure 2.

After establishing the static pressure distribution through the boundary layer at each of the 180 positions, the local velocity was calculated from total pressure measurements. Figure 3 is an example of the static pressure coefficients in the boundary layer at one position. The rake results compare favorably with the static pressure coefficient measured on the surface of the model.

DISCUSSION OF VELOCITY PROFILE MEASUREMENTS

The mean boundary layer profiles obtained by curve fitting the data points are shown in Figures 4-9. The following is the list of flow configurations for which the incoming boundary layer velocity profiles were obtained:

Figure 4 - without upstream appendages, without screen, and without rotor (Basic Flow #11)

Figure 5 - without upstream appendages, without screen, and rotor on design flow coefficient (Basic Flow #1)

Figure 6 - without upstream appendages, without screen, and rotor 10% low in flow coefficient (Basic Flow #2)

Figure 7 - without upstream appendages, with screen, and rotor on design flow coefficient (Basic Flow #3)

Figure 8 - with upstream appendages, without screen, and rotor on design flow coefficient (Basic Flow #4)

Figure 9 - with upstream appendages, with screen, and rotor on design flow coefficient (Basic Flow #7)

A comparison of the mean measurement obtained with the rotor (Figure 4) and without the rotor (Figure 5) shows that the mean velocities are higher near the rotor wall for the case with the rotor. This is particularly true near the wall where $Y << R_R$. It is probable that the higher mean velocities found with the rotor are caused by streamline convergence. This effect is produced by the favorable pressure gradient generated by the rotor.

The effect of upstream appendages can be seen by comparing Figure 5 to Figure 8. The upstream appendages consisted of four struts placed at the 0°, 90°, 180° and 270° points on the axisymmetric test body in front of the rotor. The results indicate that the upstream appendages add momentum to the deficit region near the wall and increase the incoming velocity. This deficit is a result of the secondary flows created at the intersection of the appendages and the wall.

More details of the effect of the appendages are shown in Figures 10 through 15. These figures show the circumferential variation of velocity at various radial positions. Even at relatively large distances from the body axis, sharp depressions in the velocity profile are produced. Near the body and appendage intersection, vortices are formed which entrain fresh fluid into the immediate neighborhood of the wall and displace sluggish fluid from the boundary layer. As a result, large peaks and valleys are created.

The effect of an upstream screen can also be seen by comparing Figures 5 through 7. The screen essentially thickens the momentum deficity region near the rotor wall of the rotor inflow region.

ANALYSIS OF MEAN VELOCITY PROFILES

[A] Calculation of Boundary Layer Thickness

Detailed measurements were made in the boundary layer near the body wall whereas few measurements were made at the edge of the boundary layer. Therefore, the exact boundary layer thickness (δ) cannot be determined accurately from these data. Moreover, the boundary layer thickness is also difficult to define by any calculation scheme; therefore, the displacement thickness (δ^*) and momentum thickness (θ) will be employed as more meaningful parameters for describing this flow.

Thus, the boundary layer data were analyzed to obtain both δ^* and θ for the two-dimensional axisymmetric flow. The results are shown in Tables 2 and 3.

The two-dimensional boundary layer results (Table 2) were obtained by integrating the following relationships

$$\overline{\delta^*} = \int_0^{\delta} \left(1 - \frac{U}{V_\infty}\right) dY \quad , \quad \overline{\theta} = \int_0^{\delta} \frac{U}{V_\infty}\left(1 - \frac{U}{V_\infty}\right) dY \quad , \tag{1}$$

? use U_e instead of V_∞

where Y is the distance perpendicular to the body surface. These two thicknesses define a shape factor ($\overline{H}$) given by

$$\overline{H} = \frac{\overline{\delta^*}}{\overline{\theta}} \quad . \tag{2}$$

Furthermore, an estimate of the boundary layer thickness can be made by approximating the velocity profile by a power law profile of the form

$$\frac{U}{V_\infty} = \left\{\frac{Y}{\overline{\delta}}\right\}^{1/m} \quad , \tag{3}$$

where

$$\overline{\delta} = \left\{\frac{\overline{H}(\overline{H}+1)}{\overline{H}-1}\right\} \overline{\theta} \quad , \tag{4}$$

and

$$m = \frac{2}{\overline{H}-1} \quad . \tag{5}$$

On the other hand, the turbulent boundary layer is thick and axisymmetric so the appropriate axisymmetric definitions for displacement and momentum thickness are

for thin b.l.'s

$$\delta^* = \int_0^{\delta} \left(1 - \frac{U}{V_\infty}\right) \frac{r}{r_o} dY \quad , \quad \theta = \int_0^{\delta} \frac{U}{V_\infty}\left(1 - \frac{U}{V_\infty}\right) \frac{r}{r_o} dY \quad . \tag{6}$$

A schematic of the coordinate system is shown in Figure 16. Patel [3] has shown that the relationships between planar definitions and the axisymmetric definitions of the boundary layer parameters are

$$\frac{\delta^*}{\bar{\theta}} = \bar{H} + \alpha(\bar{H} + 1) \quad , \quad \frac{\theta}{\bar{\theta}} = 1 + 2\alpha \quad ,$$

$$H = \frac{\bar{H} + \alpha(\bar{H} + 1)}{1 + 2\alpha} \quad , \tag{7}$$

where

$$\alpha = 1/2 \cos \phi \frac{\bar{\theta}}{r_o} \left\{\frac{\bar{H}^2(\bar{H} + 1)}{(\bar{H}-1)(\bar{H}+3)}\right\} \quad . \tag{8}$$

Estimates of the axisymmetric boundary layer are given in Table 3.

The results of the boundary layer analysis parallel the conclusions from Figure 4 to Figure 9. That is (1) the screen increases the momentum thickness, (2) the upstream appendages increase the momentum thickness, and (3) operating the rotor at less than the design flow coefficient decreases the momentum thickness. In all cases, the rotor operated within the estimated incoming boundary layer.

[B] Calculation of Normal Vorticity

The slope of the incoming boundary layer determines the amount of vorticity entering the rotor. The nondimensional normal vorticity is defined as

$$\omega_n = \frac{d(U/V_\infty)}{d(Y/R_R)} \quad , \tag{9}$$

where U/V_∞ is the boundary layer velocity profile, Y is the distance from the wall and R_R is the radius of the rotor. The radius of the rotor was chosen as the normalizing parameter because of the uncertainty of the boundary layer thickness.

The normal vorticity data obtained from the velocity profiles are shown in Figures 5 through 9 and are listed in Tables 4 through 8. The important conclusion is that for the average profile the upstream appendages reduce the amount of normal vorticity entering the rotor as compared to the no appendage case. This result occurs at the rotor design flow coefficient.

[C] Comparisons with Two-Dimensional Theory

Experiments with axisymmetric boundary layers as shown by Patel, Nakayoma, and Damian [6] indicate that even when the boundary layer is thick, the velocity profiles do not deviate appreciably from the two-parameter families of shape factor and Reynolds number constructed primarily for thin boundary layers. This fact applies only if the integral parameters involved are evaluated according to the usual two-dimensional boundary layer definitions. In view of this, the skin friction law for a thick axisymmetric boundary layer may be written as

$$C_f = C_f(\bar{H}, \bar{R}_o) \quad , \tag{10}$$

where the bars denote values obtained purely from the shape of the velocity profile. Thus, the friction law of Thompson [7] can be used to calculate the skin friction coefficient as outlined in Patel [3].

The shear velocity (u^*) is a simple function of the skin friction coefficient. The shear velocity is used to normalize the profile velocity. As a result, the measured velocity profile without the rotor can be represented by various boundary layer laws.

Because of the unknown boundary layer thickness, only the region near the wall can be analyzed. In this region where the vorticity is concentrated, the wall is expressed as

$$u^+ = A \log_{10} y^+ + B \quad , \quad 0.01\delta \leq y \leq 0.2\delta \quad , \tag{11}$$

where

δ - boundary layer thickness

A - slope of the logarithmic velocity law, 5.76

k - von Karman constant, 0.4

B - constant for inner logarithmic velocity law, 5.5

can be used to match the boundary layer profile.

A shear velocity of 1.6 ft/sec was determined by using Equation (10) for the skin friction coefficient. The results are shown in Figure 17 for the inner region and good agreement with the normalized planar boundary layer was found. It is interesting to note that using the planar boundary layer definitions, the shape factor ($\overline{H}$) is 1.78 indicating that the profile is near separation but the measured results do not indicate separation. This result can be expected near the tail of an axisymmetric body where the curvature effect not only dominates the boundary layer thickness but also keeps the boundary layer from separating.

SUMMARY

The incoming boundary layer profile to a rotor was measured near the body wall for various flow conditions. The analysis show that the vorticity in the boundary layer varies greatly with small changes in the boundary layer structure. As a result, the loading of the rotor near the root and the generation of secondary flows will differ even though the performance of the rotor will not change significantly.

REFERENCES

[1] Squire, H. B. and Winter, K. G., "The Secondary Flow in a Cascade of Airfoils in a Non-Uniform Stream," J. Aeronaut. Sci., Vol. 18, 1951, p. 271.

[2] Lakshminarayana, B. and Horlock, J. H., "Generalized Expressions for Secondary Vorticity Using Intrinsic Coordinates," J. Fluid Mech., Vol. 59, 1973, pp. 97-115.

[3] Patel, V. C., "A Simple Integral Method for the Calculation of Thick Axisymmetric Turbulent Boundary Layers," Aeronautical Quarterly, Vol. 25, February 1974.

[4] Patel, V. C., "On the Equation s of a Thick Axisymmetric Turbulent Boundary Layer," Iowa Institute of Hydraulic Research, Report 143, 1973.

[5] Granville, P. S., "The Calculation of the Viscous Drag of Bodies of Revolution," David Taylor Model Basin, Report 849, July 1953.

[6] Patel, V. C., Nakayama, A., and Damian, R., "An Experimental Study of the Thick Turbulent Boundary Layer Near the Tail of a Body of Revolution," Iowa Institute of Hydraulic Research, Report 142, 1973.

[7] Thompson, B. G. J., "A New Two-Parameter Family of Mean Velocity Profiles for Incompressible Boundary Layers on Smooth Walls," ARC R&M 3463, 1965.

Table 1

Basic Flow Configurations

Number	Upstream Appendages**	Upstream Screen	Rotor Flow Coefficient (ϕ)
1	No	No	$\phi=\phi_d$*
2	No	No	$\phi=0.9\phi_d$
3	No	Yes	$\phi=\phi_d$
4	Yes	No	$\phi=\phi_d$
5	Yes	No	$\phi=1.1\phi_d$
6	Yes	No	$\phi=0.9\phi_d$
7	Yes	Yes	$\phi=\phi_d$
8	Yes	Yes	$\phi=0.9\phi_d$
9	No	Yes	$\phi=0.9\phi_d$
10***	Yes	No	$\phi=\phi_d$
11	No	No	no rotor
12	No	Yes	no rotor
13	Yes	No	no rotor

* ϕ_d = design flow coefficient $\equiv V_\infty/U_{TIP}$

** The upstream appendages consisted of four struts placed at the 0°, 90°, 180° and 270° points on the axisymmetric test body.

*** Downstream body configuration change.

11 October 1976
MLB:jep

Table 2

Two-Dimensional Boundary Layer Analysis

Number	Upstream Appendages	Upstream Screen	Rotor	Flow Coefficient	δ^* Inches	$\bar{\theta}$ Inches	$\bar{H}$	$\bar{m}$	Estimated $\bar{\delta}$
1	No	No	Yes	$\phi=\phi_d$	0.830	0.539	1.54	3.70	----
2	No	No	Yes	$\phi=0.9\phi_d$	0.723	0.495	1.46	4.35	----
3	No	Yes	No	$\phi=\phi_d$	0.917	0.621	1.48	4.17	----
4	Yes	No	Yes	$\phi=\phi_d$	0.880	0.580	1.52	3.85	----
7	Yes	Yes	Yes	$\phi=\phi_d$	0.972	0.645	1.51	3.92	----
11	No	No	No	-------	1.148	0.645	1.78	2.56	4.09
12	No	Yes	No	-------	1.259	0.703	1.79	2.53	4.44
13	Yes	No	No	-------	-----	-----	----	----	----

$\bar{\delta}^*$ Displacement thickness

$\bar{\theta}$ Momentum thickness

$\bar{\delta}$ Boundary Layer thickness

$\bar{H} = \bar{\delta}^*/\bar{\theta}$

11 October 1976
MLB:jep

Table 3

Axisymmetric Boundary Layer Analysis

Number	Upstream Appendages	Upstream Screen	Rotor	Flow Coefficient	δ^* Inches	θ Inches	H	m
1	No	No	Yes	$\phi=\phi_d$	1.644	1.179	1.39	5.09
2	No	No	Yes	$\phi=0.9\phi_d$	1.414	1.057	1.34	5.09
3	No	Yes	Yes	$\phi=\phi_d$	2.003	1.495	1.34	5.89
4	Yes	No	Yes	$\phi=\phi_d$	1.825	1.328	1.37	5.36
7	Yes	Yes	Yes	$\phi=\phi_d$	2.140	1.574	1.36	5.57

δ^* Displacement thickness

θ Momentum thickness

δ Boundary layer thickness

H $= \delta^*/\theta$

11 October 1976
MLB:jep

Table 4

Boundary Layer Profile Results
(Basic Flow #1)

Flow Configuration: Without Upstream Appendages
Without Upstream Screen
Rotor at Design Flow Coefficient

Y	Y/R_R	U/V_∞	$\omega_n=d(U/V_\infty)/d(Y/R_R)$
0.050	0.013	0.360	3.21
0.100	0.026	0.397	2.58
0.150	0.040	0.425	2.21
0.200	0.053	0.450	1.95
0.250	0.066	0.468	1.74
0.300	0.080	0.493	1.57
0.350	0.093	0.513	1.45
0.400	0.106	0.531	1.53
0.450	0.120	0.545	1.2
0.500	0.133	0.560	1.18
0.600	0.160	0.583	1.06
0.700	0.186	0.603	0.98
0.800	0.213	0.622	0.91
0.900	0.240	0.640	0.87
1.000	0.266	0.658	0.92
1.100	0.293	0.677	0.78
1.200	0.320	0.695	0.76
1.300	0.346	0.715	0.73
1.400	0.373	0.732	0.71
1.500	0.400	0.750	0.70
1.600	0.426	0.768	0.68
1.700	0.453	0.785	0.66
1.800	0.480	0.802	0.64
1.900	0.506	0.816	0.63
2.000	0.533	0.834	0.61
2.100	0.560	0.850	0.58
2.200	0.586	0.862	0.56
2.300	0.613	0.875	0.54
2.400	0.640	0.887	0.51
2.500	0.666	0.897	0.49
2.600	0.693	0.907	0.46
2.700	0.720	0.917	0.44
2.800	0.746	0.927	0.42
2.900	0.773	0.935	0.39
3.000	0.800	0.943	0.36
3.100	0.826	0.950	0.34
3.200	0.853	0.955	0.31
3.300	0.880	0.961	0.29
3.400	0.906	0.967	0.26
3.500	0.986	0.973	0.23
3.600	0.960	0.977	0.21
3.700	0.986	0.981	0.18
3.800	1.013	0.985	0.15

Table 5

Boundary Layer Profile Results
(Basic Flow #2)

Flow Configuration: Without Upstream Appendages
Without Upstream Screen
Rotor at 0.9 Design Flow Coefficient

Y	Y/R_R	U/V_∞	$\omega_n = d(U/V_\infty)/d(Y/R_R)$
0.050	0.013	0.410	3.11
0.100	0.026	0.445	2.67
0.150	0.040	0.475	2.32
0.200	0.053	0.500	2.02
0.250	0.066	0.523	1.78
0.300	0.080	0.542	1.57
0.350	0.093	0.561	1.39
0.400	0.106	0.576	1.25
0.450	0.120	0.590	1.15
0.500	0.133	0.604	1.06
0.600	0.160	0.638	0.93
0.700	0.186	0.650	0.84
0.800	0.213	0.669	0.79
0.900	0.240	0.685	0.76
1.000	0.266	0.704	0.75
1.100	0.293	0.721	0.73
1.200	0.320	0.738	0.72
1.300	0.346	0.755	0.71
1.400	0.373	0.770	0.69
1.500	0.400	0.785	0.67
1.600	0.426	0.802	0.65
1.700	0.453	0.816	0.63
1.800	0.480	0.832	0.61
1.900	0.506	0.847	0.59
2.000	0.533	0.860	0.57
2.100	0.560	0.873	0.54
2.200	0.586	0.885	0.52
2.300	0.613	0.895	0.50
2.400	0.640	0.905	0.46
2.500	0.666	0.914	0.44
2.600	0.693	0.924	0.42
2.700	0.720	0.933	0.39
2.800	0.746	0.940	0.36
2.900	0.773	0.948	0.31
3.000	0.800	0.955	0.29
3.100	0.826	0.961	0.26
3.200	0.853	0.966	0.23
3.300	0.880	0.972	0.19
3.400	0.906	0.976	0.16
3.500	0.933	0.979	0.12
3.600	0.960	0.982	0.05
3.700	0.986	0.985	0.05
3.800	1.013	0.987	0.02

11 October 1976
MLB:jep

Table 6

Boundary Layer Profile Results
(Basic Flow #3)

Flow Configuration: Without Upstream Appendages
With Upstream Screen
Rotor at Design Flow Coefficient

Y	Y/R_R	U/V_∞	$\omega_n = d(U/V_\infty)/d(Y/R_R)$
0.050	0.013	0.380	3.02
0.100	0.026	0.415	2.30
0.150	0.040	0.445	2.04
0.200	0.053	0.472	1.84
0.250	0.066	0.495	1.69
0.300	0.080	0.515	1.56
0.350	0.093	0.535	1.46
0.400	0.106	0.550	1.36
0.450	0.120	0.565	1.29
0.500	0.133	0.580	1.23
0.600	0.160	0.605	1.11
0.700	0.186	0.623	1.02
0.800	0.213	0.640	0.94
0.900	0.240	0.655	0.88
1.000	0.266	0.670	0.82
1.100	0.293	0.682	0.78
1.200	0.320	0.702	0.73
1.300	0.346	0.717	0.69
1.400	0.373	0.730	0.63
1.500	0.400	0.745	0.61
1.600	0.426	0.755	0.57
1.700	0.453	0.765	0.56
1.800	0.480	0.775	0.51
1.900	0.506	0.785	0.50
2.000	0.533	0.795	0.46
2.100	0.560	0.806	0.45
2.200	0.586	0.812	0.43
2.300	0.613	0.825	0.41
2.400	0.640	0.834	0.39
2.500	0.666	0.842	0.37
2.600	0.693	0.850	0.36
2.700	0.720	0.858	0.34
2.800	0.746	0.867	0.32
2.900	0.773	0.875	0.31
3.000	0.800	0.883	0.29
3.100	0.826	0.890	0.28
3.200	0.853	0.898	0.27
3.300	0.880	0.906	0.26
3.400	0.906	0.914	0.25
3.500	0.933	0.920	0.24
3.600	0.960	0.935	0.22
3.700	0.986	0.942	0.21
3.800	1.013	0.950	0.20

11 October 1976
MLB:jep

Table 7

Boundary Layer Profile Results
(Basic Flow #4)

Flow Configuration: With Upstream Appendages
Without Upstream Screen
Rotor at Design Flow Coefficient

Y	Y/R_R	U/V_∞	$\omega_n = d(U/V_\infty)/d(Y/R_R)$
0.050	0.013	0.420	3.18
0.100	0.026	0.450	1.95
0.150	0.050	0.468	1.40
0.200	0.053	0.478	1.17
0.250	0.066	0.495	1.03
0.300	0.080	0.507	0.94
0.350	0.093	0.517	0.88
0.400	0.106	0.527	0.86
0.450	0.120	0.537	0.85
0.500	0.133	0.547	0.85
0.600	0.160	0.567	0.84
0.700	0.186	0.586	0.81
0.800	0.213	0.607	0.80
0.900	0.240	0.625	0.79
1.000	0.266	0.644	0.78
1.100	0.293	0.661	0.76
1.200	0.320	0.678	0.75
1.300	0.346	0.697	0.74
1.400	0.373	0.714	0.73
1.500	0.400	0.732	0.72
1.600	0.426	0.749	0.71
1.700	0.453	0.761	0.69
1.800	0.480	0.783	0.67
1.900	0.506	0.799	0.65
2.000	0.533	0.814	0.63
2.100	0.560	0.827	0.61
2.200	0.586	0.842	0.59
2.300	0.613	0.851	0.57
2.400	0.640	0.860	0.55
2.500	0.666	0.870	0.52
2.600	0.693	0.880	0.50
2.700	0.720	0.887	0.48
2.800	0.746	0.895	0.46
2.900	0.773	0.903	0.44
3.000	0.800	0.910	0.42
3.100	0.826	0.915	0.40
3.200	0.853	0.923	0.37
3.300	0.880	0.930	0.35
3.400	0.906	0.934	0.31
3.500	0.933	0.942	0.30
3.600	0.960	0.948	0.27
3.700	0.986	0.952	0.23
3.800	1.013	0.955	0.22

Table 8

Boundary Layer Profile Results
(Basic Flow #7)

Flow Configuration: With Upstream Appendages
With Upstream Screen
Rotor at Design Flow Coefficient

Y	Y/R_R	U/V_∞	$\omega_n = d(U/V_\infty)/d(Y/R_R)$
0.050	0.013	0.405	2.04
0.100	0.026	0.430	1.80
0.150	0.040	0.450	1.63
0.200	0.053	0.470	1.48
0.250	0.066	0.485	1.37
0.300	0.080	0.502	1.27
0.350	0.093	0.517	1.18
0.400	0.106	0.529	1.11
0.450	0.120	0.541	1.05
0.500	0.133	0.552	1.00
0.600	0.160	0.573	0.90
0.700	0.186	0.592	0.84
0.800	0.213	0.611	0.78
0.900	0.240	0.628	0.75
1.000	0.266	0.647	0.72
1.100	0.293	0.658	0.69
1.200	0.320	0.679	0.68
1.300	0.346	0.695	0.66
1.400	0.373	0.707	0.65
1.500	0.400	0.720	0.63
1.600	0.426	0.731	0.60
1.700	0.453	0.743	0.58
1.800	0.480	0.754	0.56
1.900	0.506	0.765	0.54
2.000	0.533	0.775	0.52
2.100	0.560	0.785	0.51
2.200	0.586	0.796	0.50
2.300	0.613	0.806	0.48
2.400	0.640	0.816	0.47
2.500	0.666	0.826	0.46
2.600	0.693	0.836	0.45
2.700	0.720	0.845	0.44
2.800	0.746	0.855	0.43
2.900	0.773	0.865	0.42
3.000	0.800	0.875	0.40
3.100	0.826	0.884	0.39
3.200	0.853	0.893	0.38
3.300	0.880	0.903	0.37
3.400	0.906	0.913	0.36
3.500	0.933	0.923	0.35
3.600	0.960	0.932	0.34
3.700	0.986	0.942	0.33
3.800	1.013	0.951	0.33

11 October 1976
MLB:jep

Table 9

Boundary Layer Profile Results
(Basic Flow #11)

Flow Configuration: Without Upstream Appendages
Without Upstream Screen
Without Rotor

Y	Y/R_R	U/V_∞
0.050	0.013	0.245
0.100	0.026	0.275
0.200	0.053	0.335
0.300	0.080	0.375
0.400	0.106	0.412
0.500	0.133	0.443
0.600	0.160	0.468
0.700	0.186	0.490
0.800	0.213	0.510
0.900	0.240	0.530
1.000	0.266	0.552
1.250	0.333	0.603
1.500	0.400	0.650
1.750	0.466	0.700
2.000	0.533	0.742
2.500	0.666	0.827
3.000	0.800	0.900
3.500	0.933	0.960
4.000	1.066	0.990

11 October 1976
MLB:jep

Table 10

Boundary Layer Profile Results
(Basic Flow #12)

Flow Configuration: Without Upstream Appendages
With Upstream Screen
Without Rotor

Y	Y/R_R	U/V_∞
0.050	0.013	0.225
0.100	0.026	0.295
0.200	0.053	0.354
0.300	0.080	0.395
0.400	0.106	0.430
0.500	0.133	0.450
0.600	0.160	0.468
0.700	0.186	0.485
0.800	0.213	0.503
0.900	0.240	0.517
1.000	0.266	0.534
1.250	0.333	0.568
1.500	0.400	0.610
1.750	0.466	0.655
2.000	0.533	0.695
2.500	0.666	0.780
3.000	0.800	0.855
3.500	0.933	0.935
4.000	1.066	0.999

Table 11

Boundary Layer Profile Results
(Basic Flow #13)

Flow Configuration: With Upstream Appendages
Without Upstream Screen
Without Rotor

Y	Y/R_R	U/V_∞
0.050	0.013	0.325
0.100	0.026	0.356
0.200	0.053	0.383
0.300	0.080	0.390
0.400	0.106	0.405
0.500	0.133	0.410
0.600	0.160	0.420
0.700	0.186	0.435
0.800	0.213	0.455
0.900	0.240	0.475
1.000	0.266	0.500
1.250	0.333	0.545
1.500	0.400	0.590
1.750	0.466	0.635
2.000	0.533	0.675
2.500	0.666	0.755
3.000	0.800	0.830
3.500	0.933	0.900
4.000	1.066	0.940

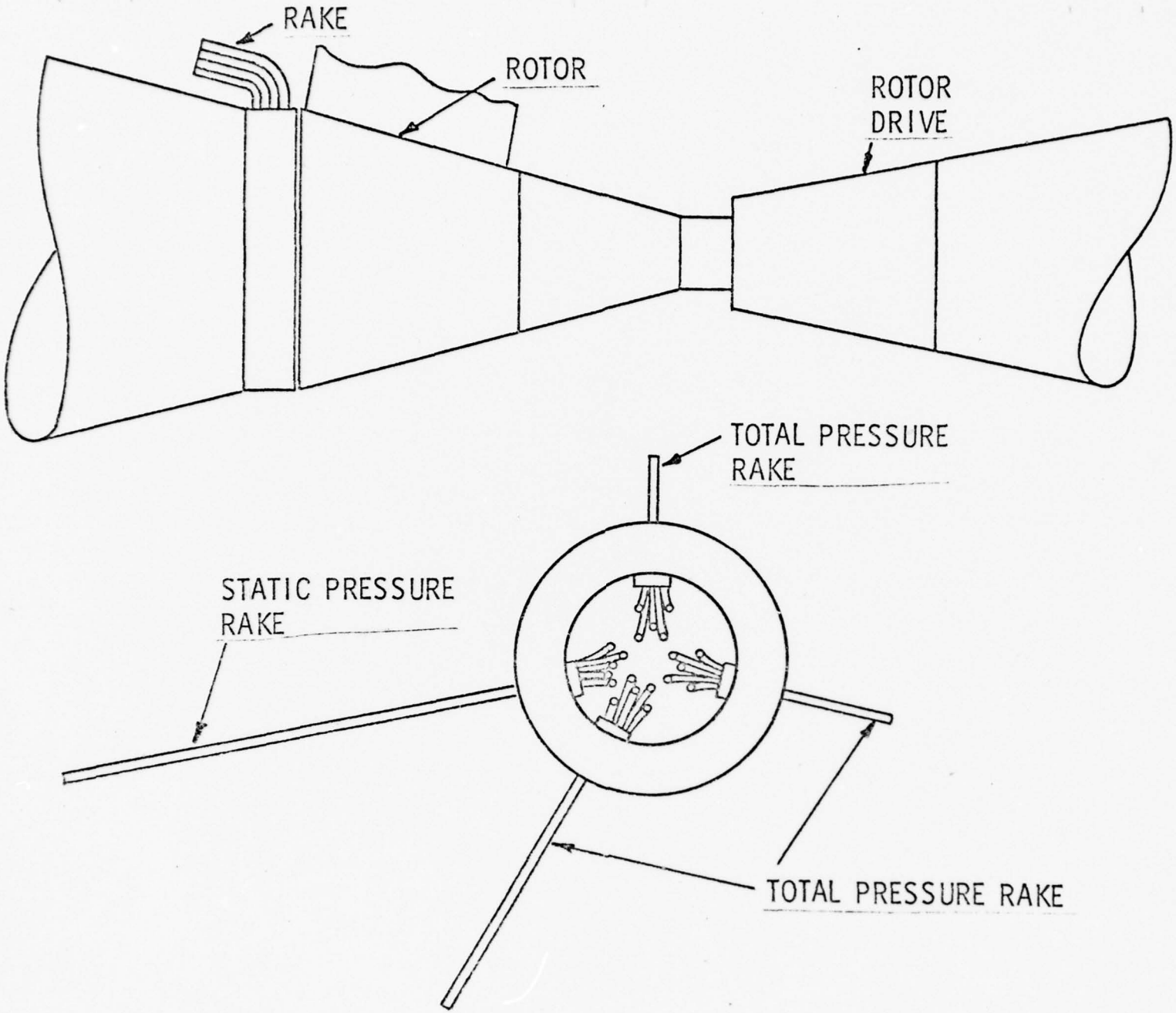

Figure 1 - Schematic of Wind Tunnel Set-Up

11 October 1976
MLB:jep

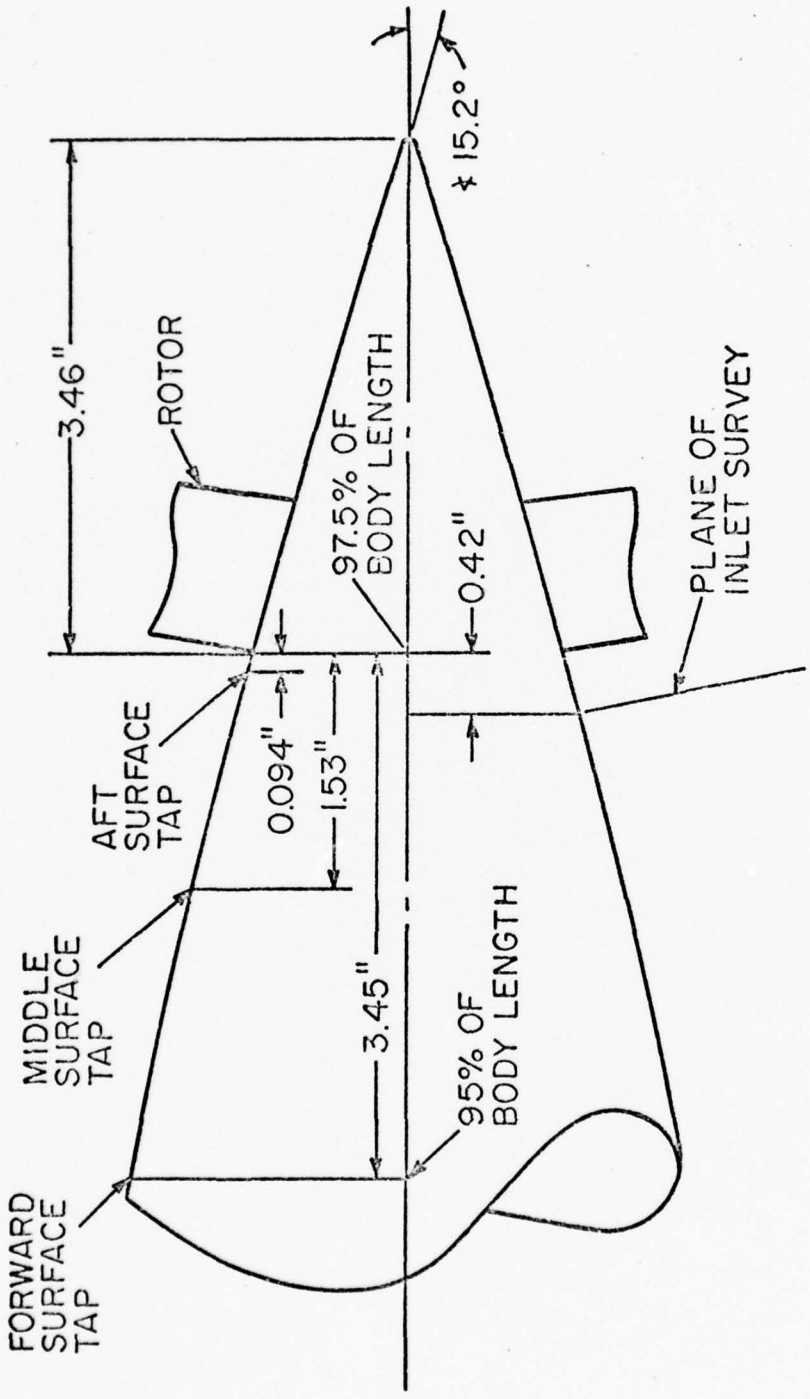

Figure 2 - Schematic of Static Pressure Locations

11 October 1976
MLB:jep

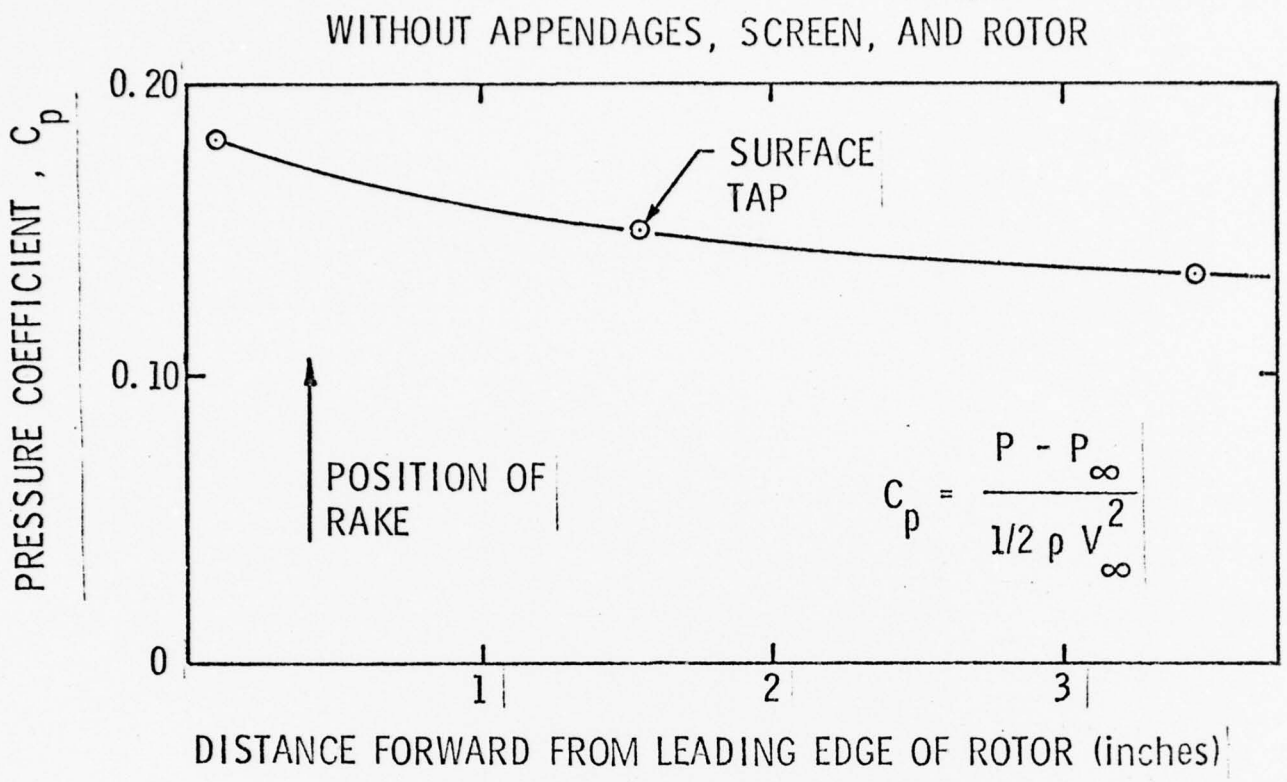

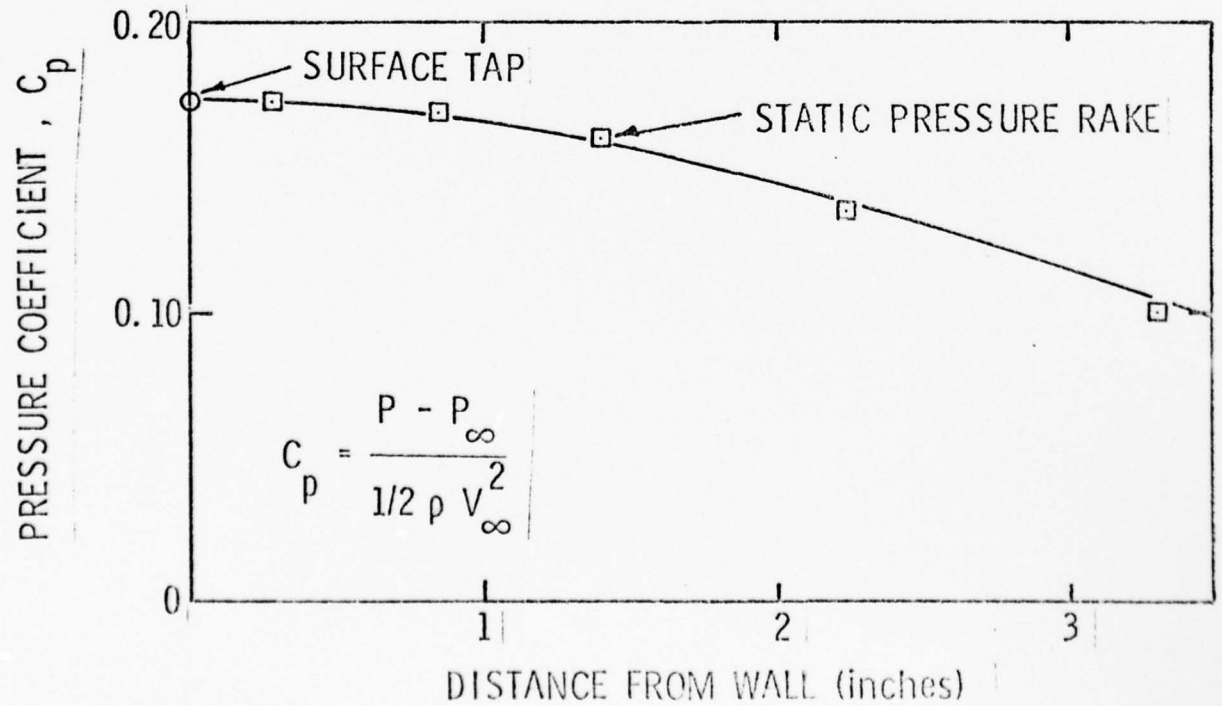

Figure 3 - Static Pressure Distribution for Boundary Layer Thickness Larger than Body Radius

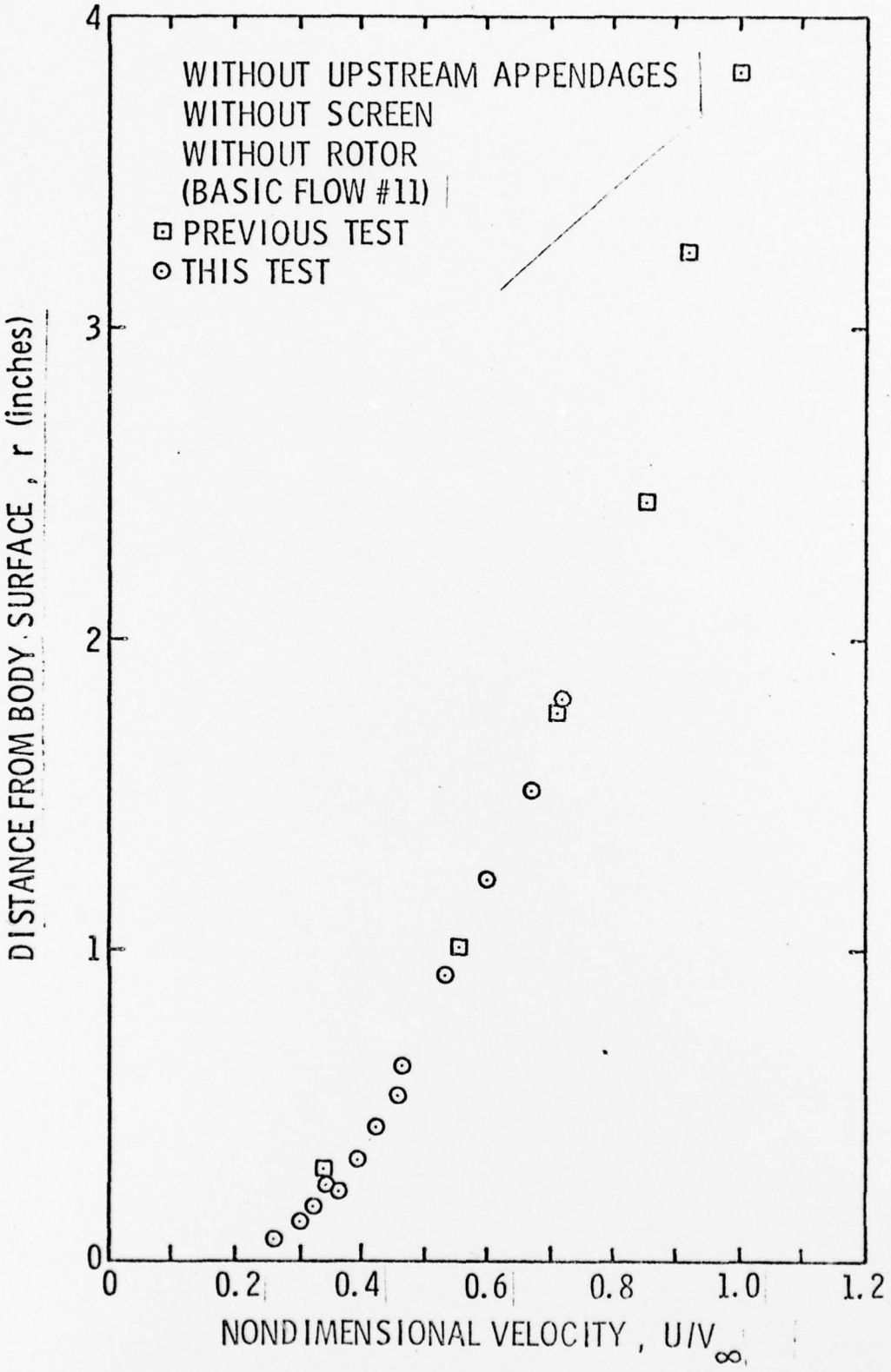

Figure 4 - Boundary Layer Profile without Appendages, Screen, and Rotor (Basic Flow #11)

11 October 1976
MLB:jep

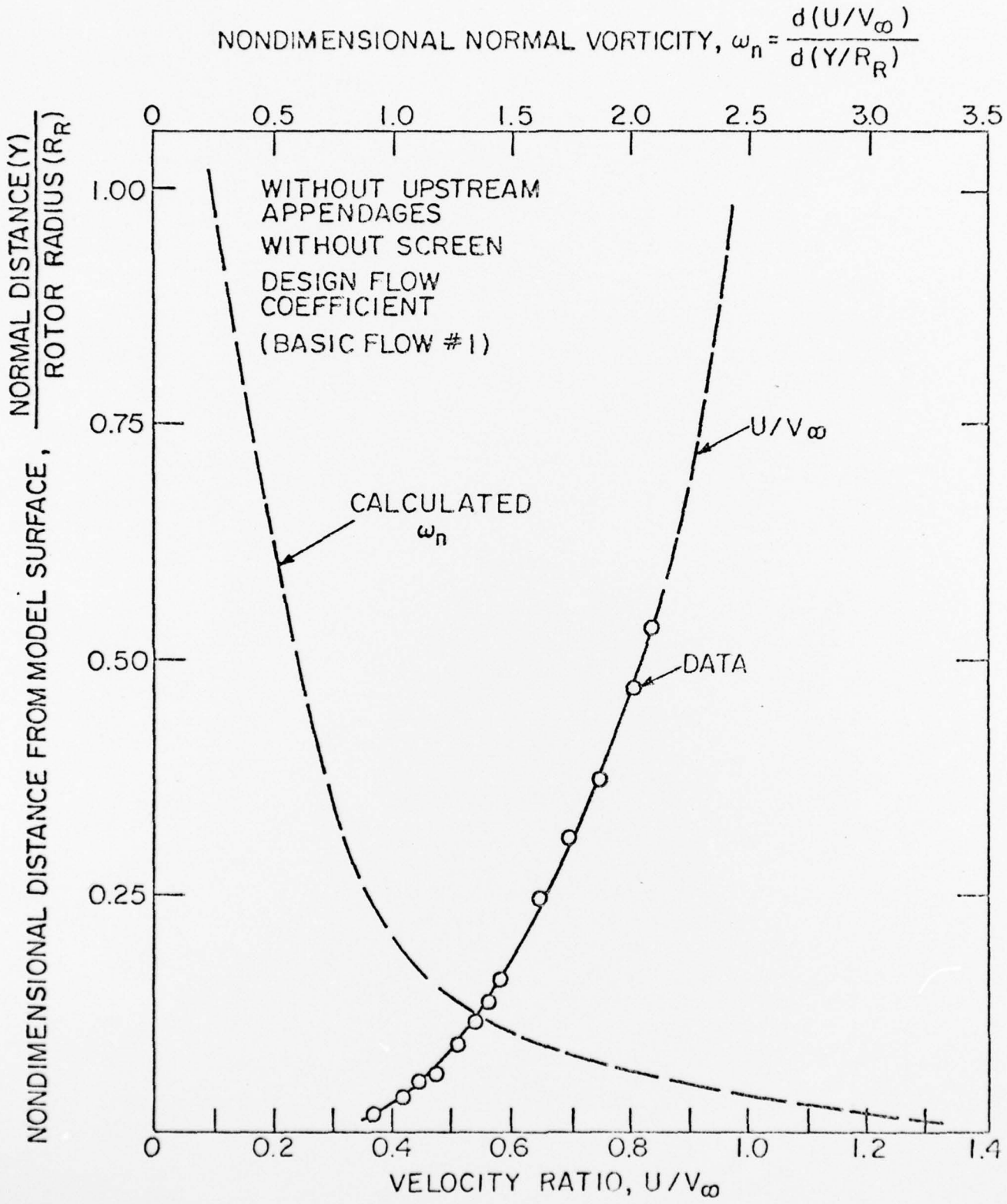

Figure 5 - Boundary Layer Profile without Upstream Appendages, without Screen, and Rotor at Design Flow Coefficient (Basic Flow #1)

11 October 1976
MLB:jep

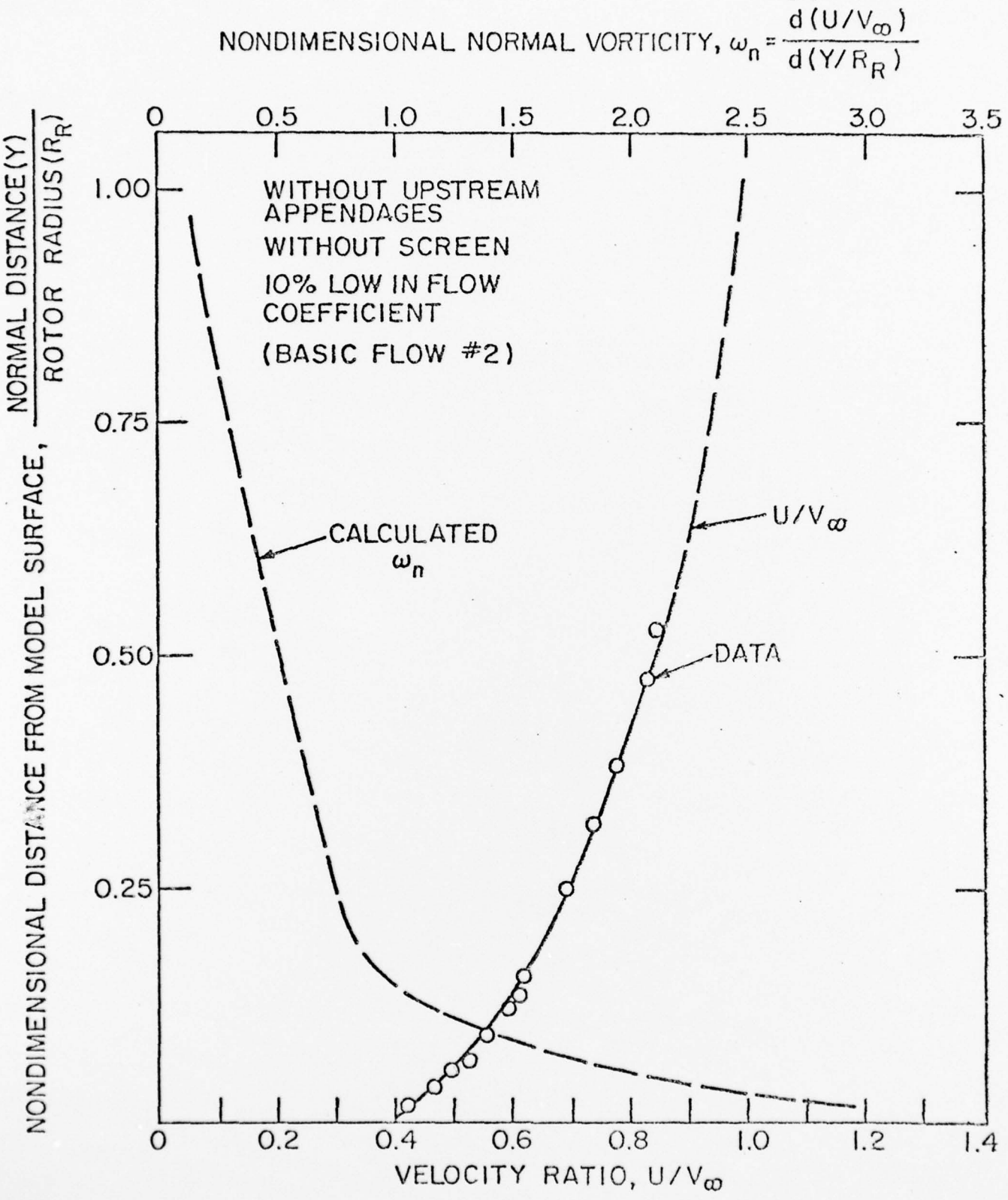

Figure 6 - Boundary Layer Profile without Upstream Appendages, without Screen, and Rotor at 0.90 Design Flow Coefficient (Basic Flow #2)

11 October 1976
MLB:jep

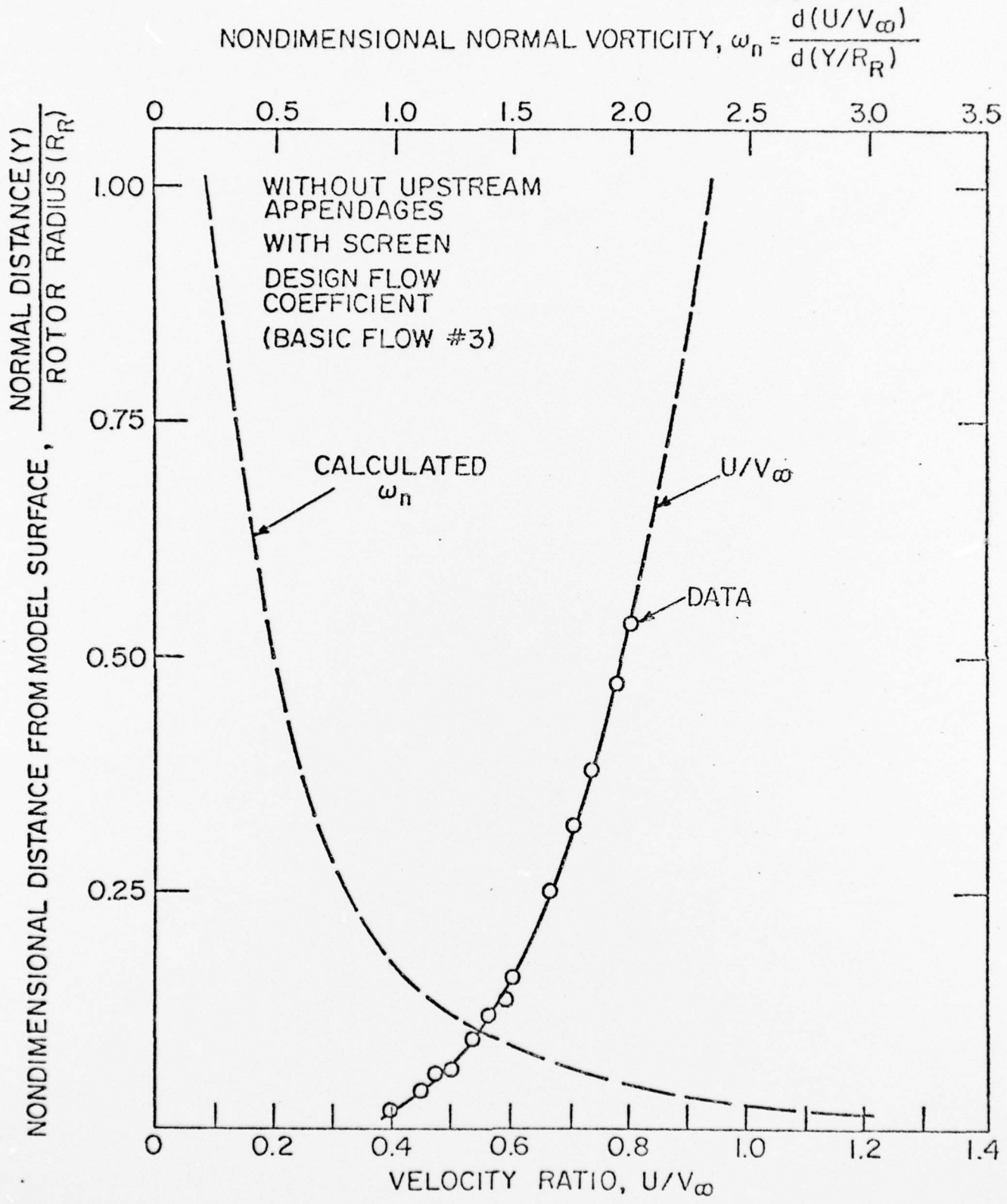

Figure 7 - Boundary Layer Profile without Upstream Appendages, with Screen, and Rotor at Design Flow Coefficient (Basic Flow #3)

11 October 1976
MLB:jep

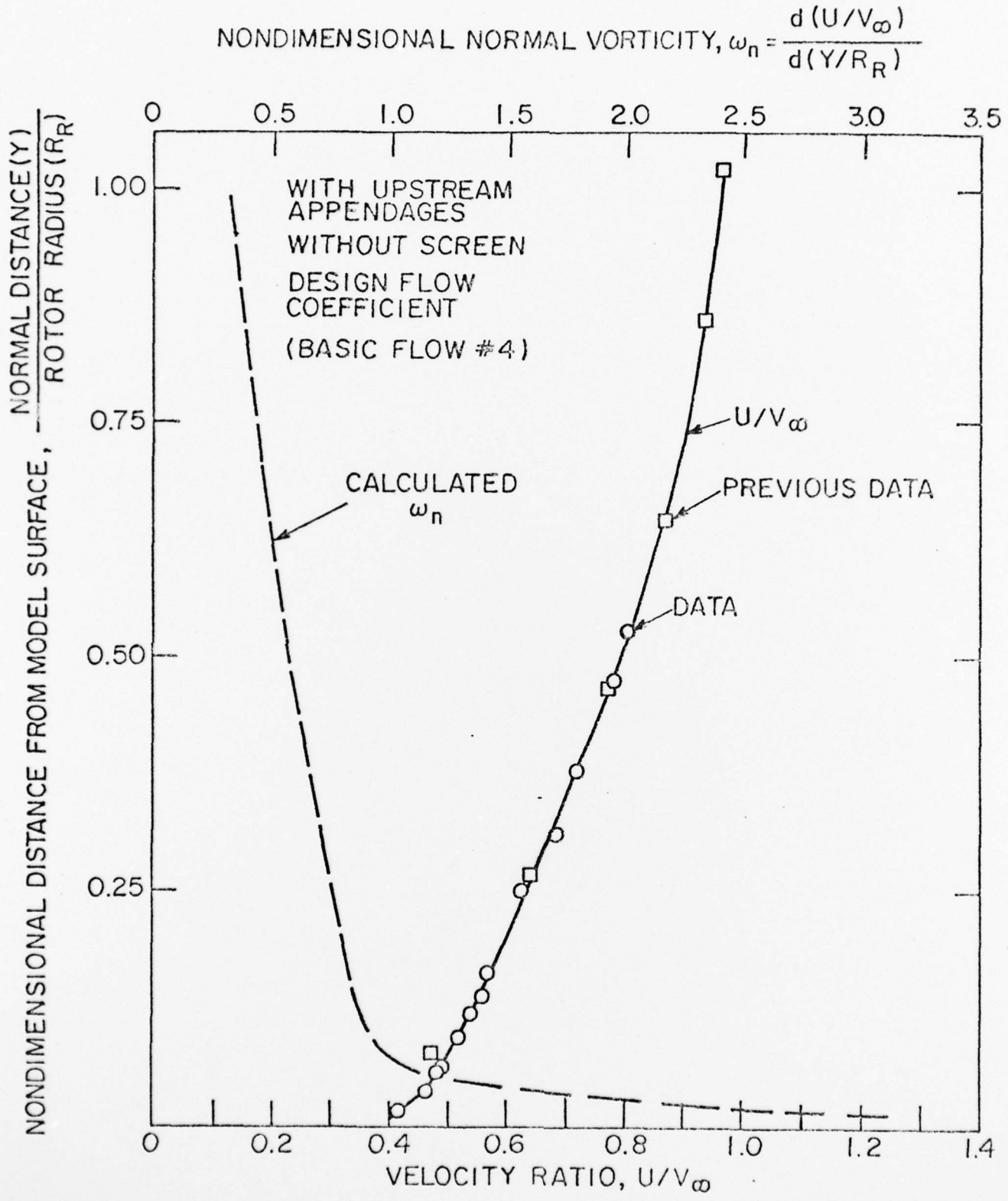

Figure 8 - Boundary Layer Profile with Upstream Appendages, without Screen, and Rotor at Design Flow Coefficient (Basic Flow #4)

11 October 1976
MLB:jep

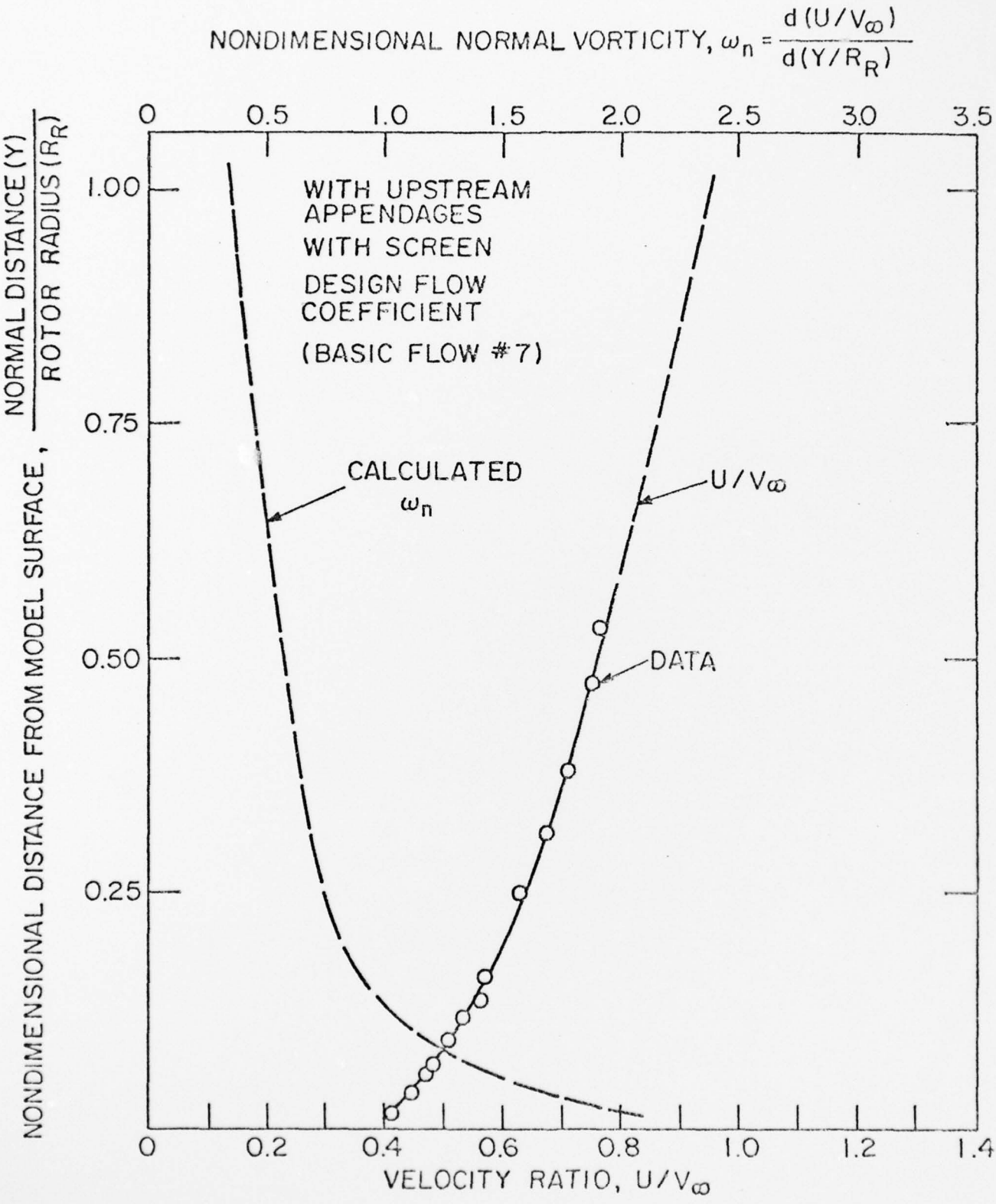

Figure 9 - Boundary Layer Profile with Upstream Appendages, with Screen, and Rotor at Design Flow Coefficient (Basic Flow #7)

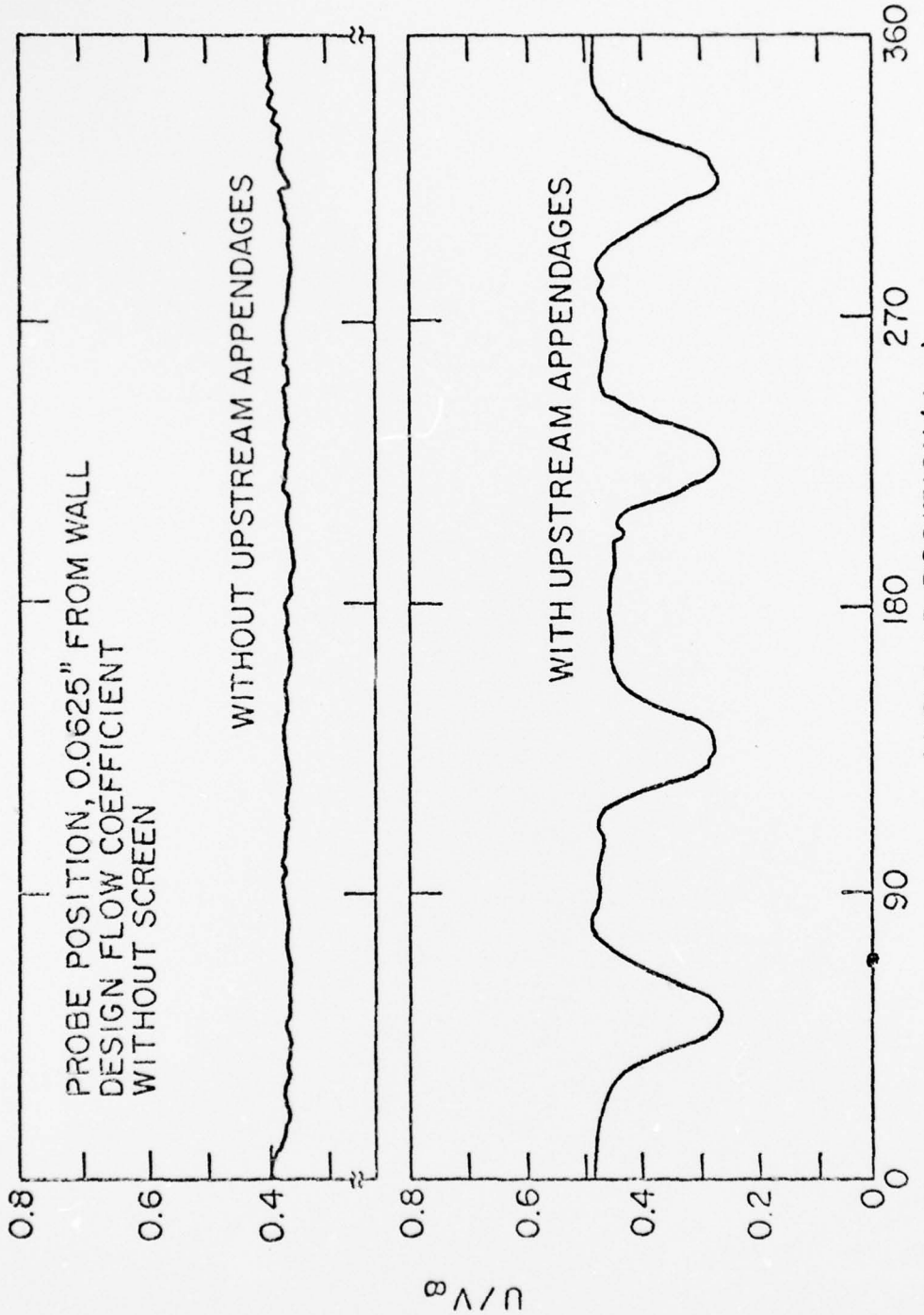

Figure 10 - Comparison of Axial Velocity Measured 0.0625 Inches from Wall with and without Upstream Appendages

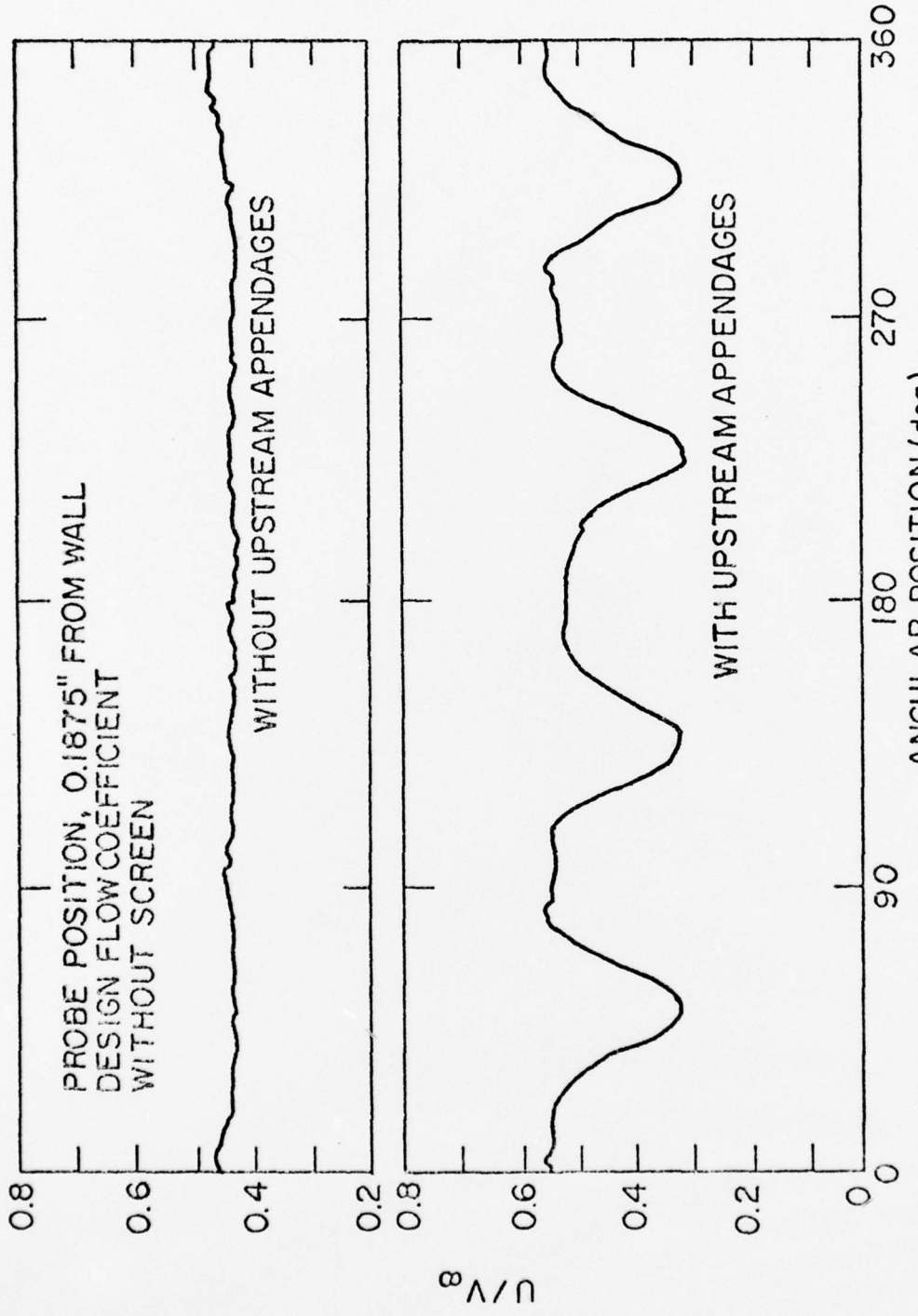

Figure 11 - Comparison of Axial Velocity Measured 0.1875 inches from Wall with and without Upstream Appendages

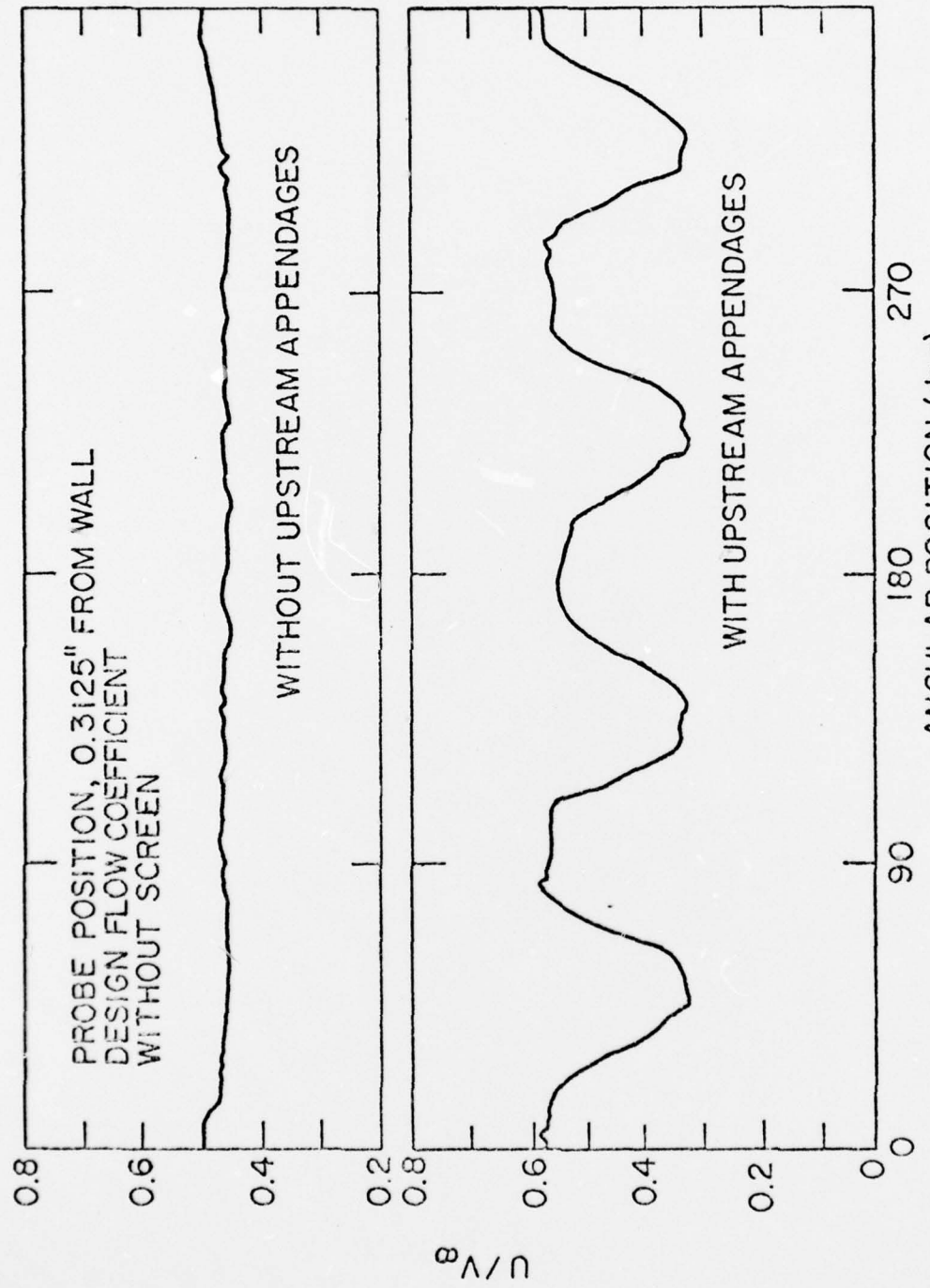

Figure 12 - Comparison of Axial Velocity Measured 0.3125 inches from Wall with and without Upstream Appendages

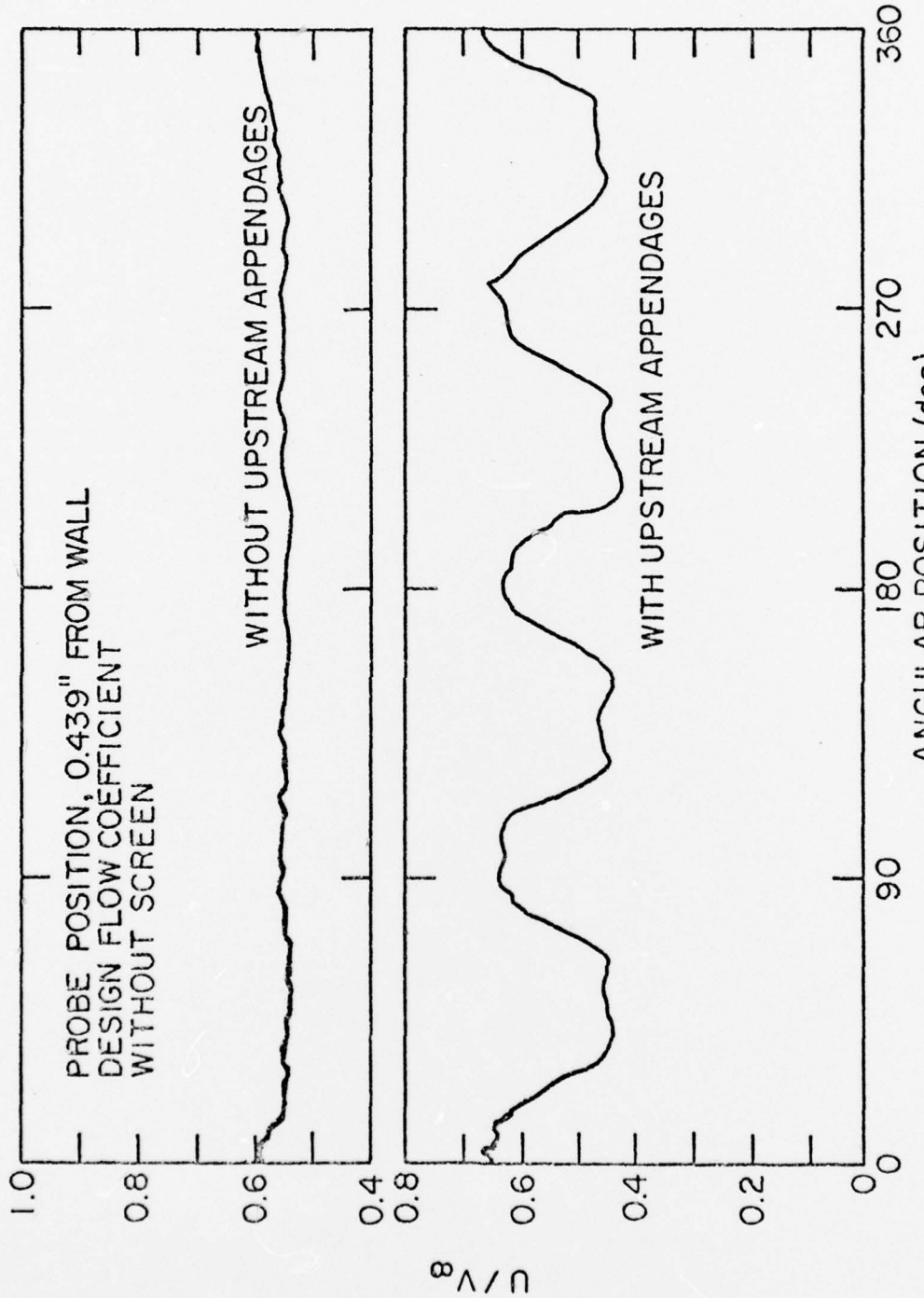

Figure 13 - Comparison of Axial Velocity Measured 0.439 inches from Wall with and without Upstream Appendages

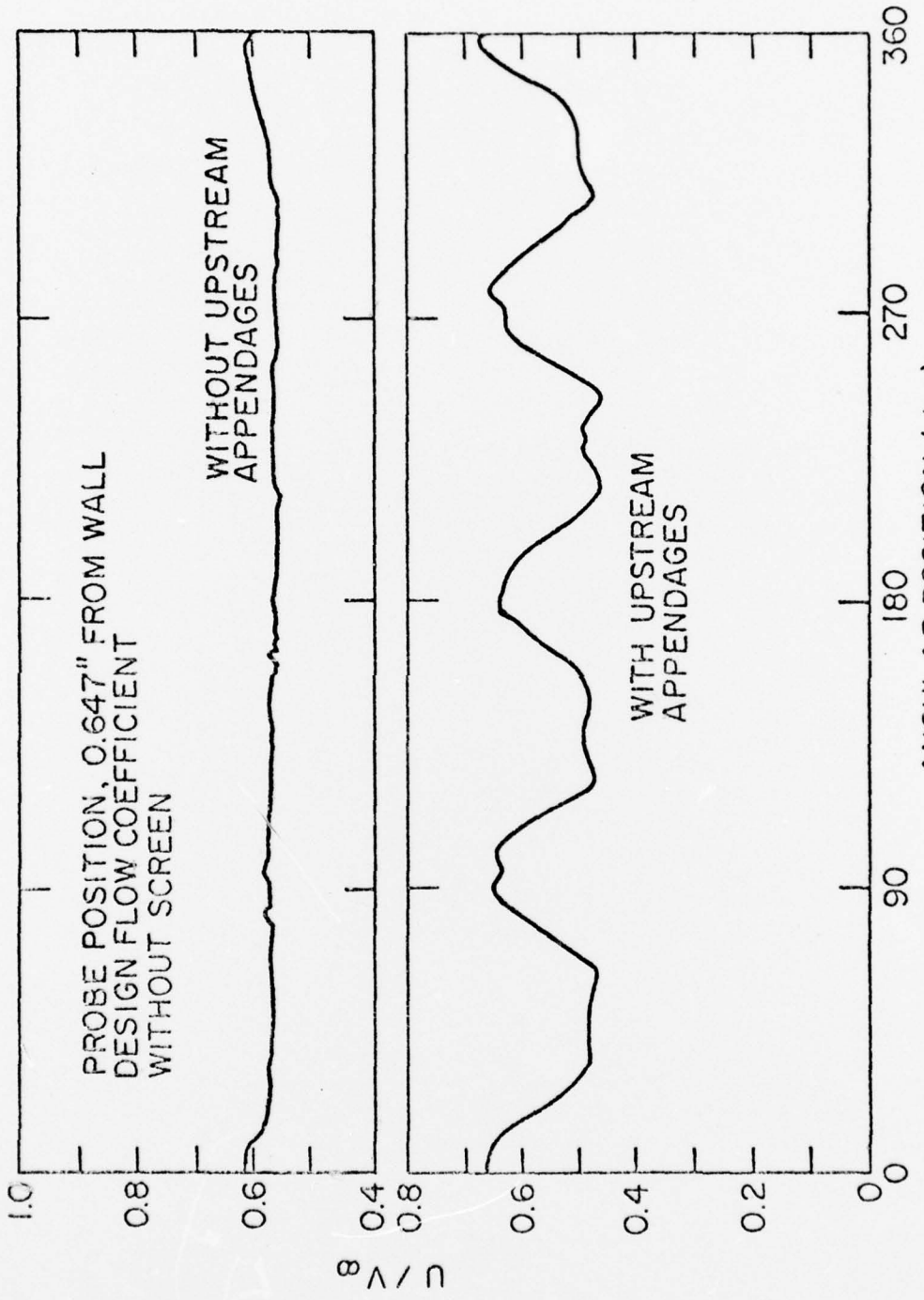

Figure 14 - Comparison of Axial Velocity Measured 0.647 inches from Wall with and without Upstream Appendages

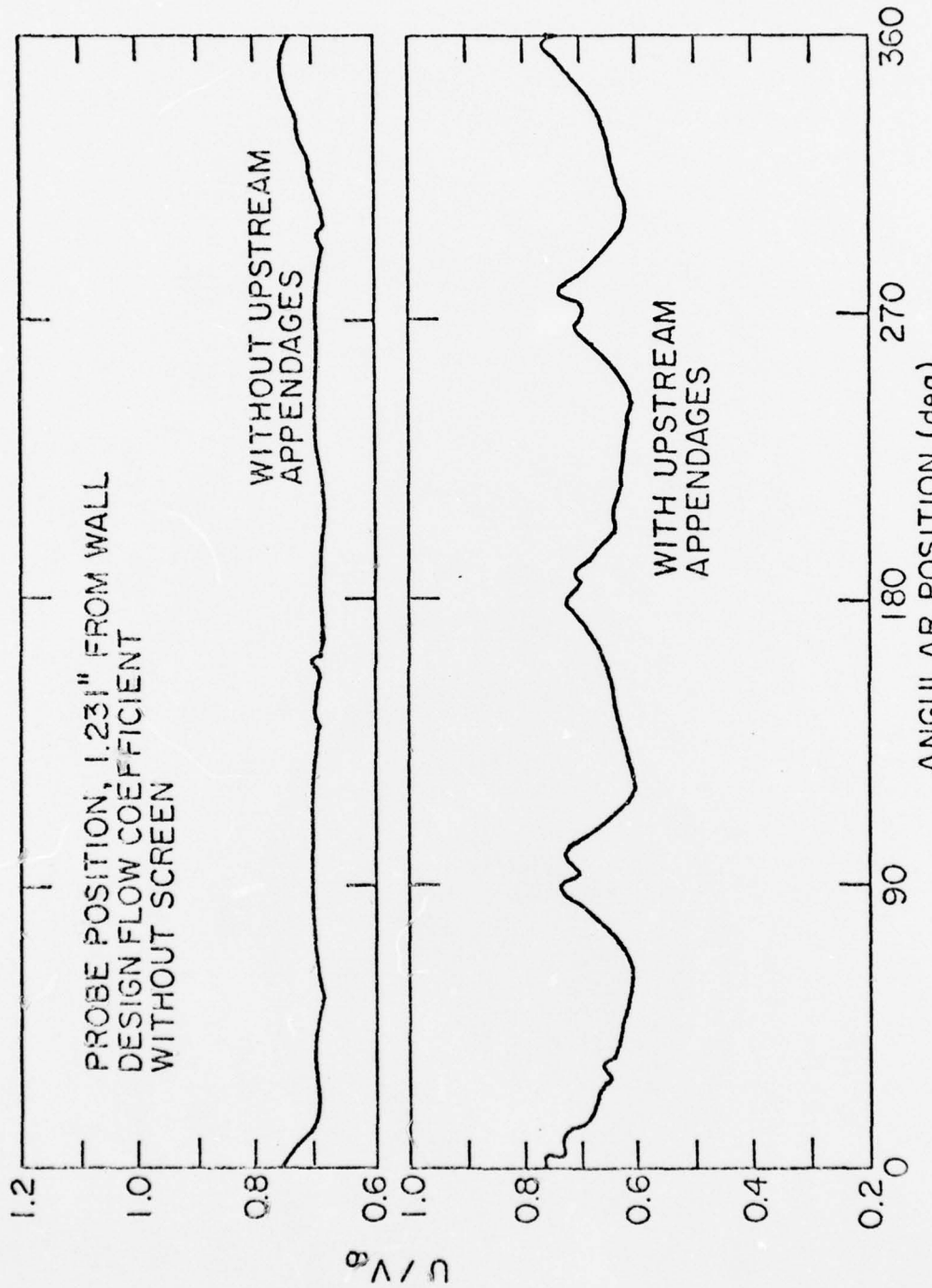

Figure 15 - Comparison of Axial Velocity Measured 1.231 inches from Wall with and without Upstream Appendages

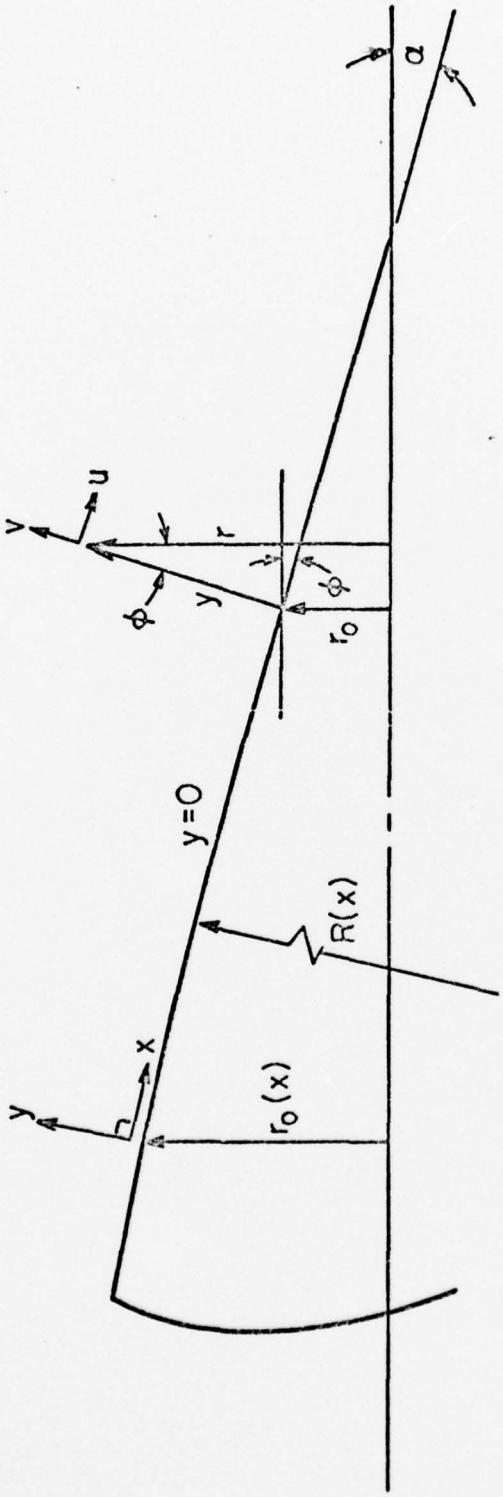

Figure 16 - Schematic of Axisymmetric Coordinate System

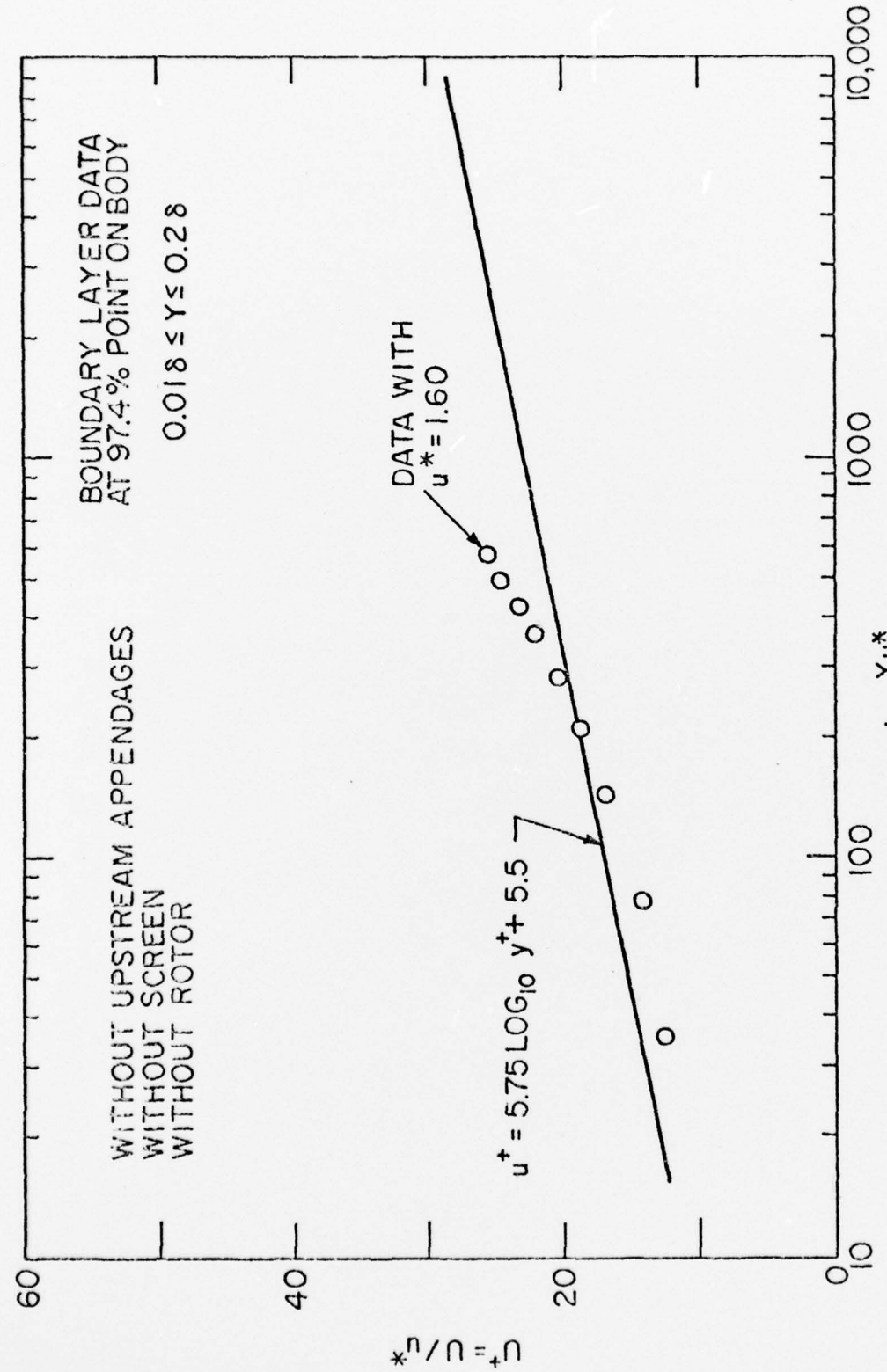

Figure 17 - Analysis of Boundary Layer Profile for $0.1\delta \leq Y \leq 0.2\delta$